Supporting Information

Engineering of Defective MOF-801 Nanostructures on the Surface of Calcium Alginate Aerogel for Efficient and Stable Atmospheric Water Harvesting

Cai-Hua Liu[1], Lei Xu[1*], Zhen-Yu Wang[1], Sheng-Jie Han[1], Yi-Bin Li[1], Ming-Lai Fu[1*], Baoling Yuan[1,2*]

[1]*Xiamen Key Laboratory of Municipal and Industrial Solid Waste Utilization and Pollution Control, College of Civil Engineering, Huaqiao University, Xiamen, Fujian 361021, P.R. China*

[2]*Key Laboratory of Songliao Aquatic Environment, Ministry of Education, Jilin Jianzhu University, Changchun, 130118, P.R. China*

*Corresponding authors. Tel: +86 592 616 2780

E-mail address: mlfu@hqu.edu.cn; lxu@hqu.edu.cn; yuanbl@hotmail.com

Text S1.

The water adsorption capacity of the samples was evaluated based on the change in real-time mass from the initial mass, and the following formula was used to calculate the amount of water adsorbed:

$$B = \frac{m_e - m_s}{m_s} \tag{S1}$$

where B denotes the amount of water adsorbed by the water-collecting material in the experiment (g·g^{-1}), m_s denotes the initial dry weight of the water collecting material (g), and m_e denotes the total mass of water vapor after adsorption (g).

The desorption rate of water in the experiment can be calculated by the following equation:

$$\eta = \frac{m_e - m_i}{m_e - m_s} \tag{S2}$$

where η is the desorption rate of water in the desorption experiment, m_s denotes the initial dry weight of the water collecting material (g), m_e denotes the total mass of water vapor after adsorption (g), and m_i is the real-time mass of the sample during desorption (g).

Text S2. Calculation method of defects in MOF-801 and MOF-801-G.

Thermogravimetric (TG) tests were performed according to reported methods to analyze the chemical structure of MOF.[1-3] The oxidative decomposition of defect-free MOF-801 follows the following chemical reaction equation, assuming complete decomposition of MOF-801 to ZrO_2 at 650 °C:

$$Zr_6O_6\left(C_4H_4O_4\right)_6\,(s) + 20O_2\,(g) \rightarrow 6ZrO_2\,(s) + 24CO_2\,(g) + 12H_2O\,(g) \qquad (S3)$$

Therefore, six equivalents of ZrO_2 are produced for each equivalent of $Zr_6O_6(FA)_6$.

When the solvents were formic acid, respectively, the defectivity of the MOF-801 structure was calculated as follows:

$$Zr_6O_6\left(C_4H_4O_4\right)_{6-x}(CH_2O_2)_{2x}\,(s) + (15-x)O_2\,(g) \rightarrow 6ZrO_2\,(s) + (24-2x)CO_2\,(g) + 12H_2O\,(g) \qquad (S4)$$

where x is the number of missing ligands at the MOF-801 defective site. According to Eq. S4, similar to that of the defect-free Zr-MOF, in the case of complete disassembly, each equivalent of Zr-MOF, i.e., MOF-801 and MOF-801-G, would be converted to six equivalents of ZrO_2. The ratio of the theoretical Zr-MOF mass to the mass of the six of ZrO_2 (remaining ash) was calculated. These values were then compared to the experimental mass loss and the value of x was calculated. The calculated values of x in MOF-801 and MOF-801-G were 0.453 and 2.748, respectively.

Text S3.

Water vapor adsorption isotherms were determined on MOF-801-G and P0.5MC aerogels using a Micromeritics ASAP 2460 instrument. The adsorption isotherms of water vapor (with P0 values of 3.157 kPa and 5.60 kPa, respectively) were measured in the vapor state at temperatures of 25 °C (298 K) and 35 °C (308 K). The heat of adsorption was calculated from the following *Clausius-Clapeyron* equation.

$$Q_{st} = \frac{RT_1T_2}{T_2 - T_1}(\ln P_2 - \ln P_1) \quad \text{(S5)}$$

where Q_{st} is the heat of adsorption (J mol^{-1}), R is the ideal gas constant (8.134 J mol^{-1} K^{-1}), T_1 and T_2 denote the temperature of the system at two different temperatures (K), and P_1 and P_2 denote the saturated vapor pressure of water vapor at two different temperatures.

Text S4. Calculation of the equivalent evaporation enthalpy of water in gels.

$$U_{in} = h_{vap} \times m_0 = h_g \times m_g \tag{S6}$$

where U_{in} (J) is the equivalent enthalpy of evaporation of water inside the gel; h_{vap} and h_g ($J \cdot g^{-1}$) are the enthalpies of evaporation of pure water and water inside the gel, respectively; and m_0 and m_g (g) are the mass changes of pure water and water inside the gel, respectively, at dark.

Text S5. Calculation of the solar vapor conversion efficiency of the gels.

$$\eta = \frac{m(L_v + Q)}{P_{in}} \tag{S7}$$

$$Q = C(T_1 - T_2) \tag{S8}$$

where η is the solar vapor conversion efficiency. m (kg·m^{-2}·h^{-1}) is the unit mass flow of the water body under light, which is equal to the difference between the mass flow of the evaporation system under light (m_{light}) and without light (m_{dark}). L_v (kJ·kg^{-1}) is the latent heat of vaporization of water, normally 2256 kJ·kg^{-1} is used in the region of interest, Q (kJ·kg^{-1}) is the energy provided to heat the system from the initial temperature T_1 (°C) to a final temperature T_2 (°C), C is the specific heat capacity of water (4.2 kJ·°C^{-1}·kg^{-1}),and P_{in} (kW·m^{-2})is the incident light power on the solar absorber.

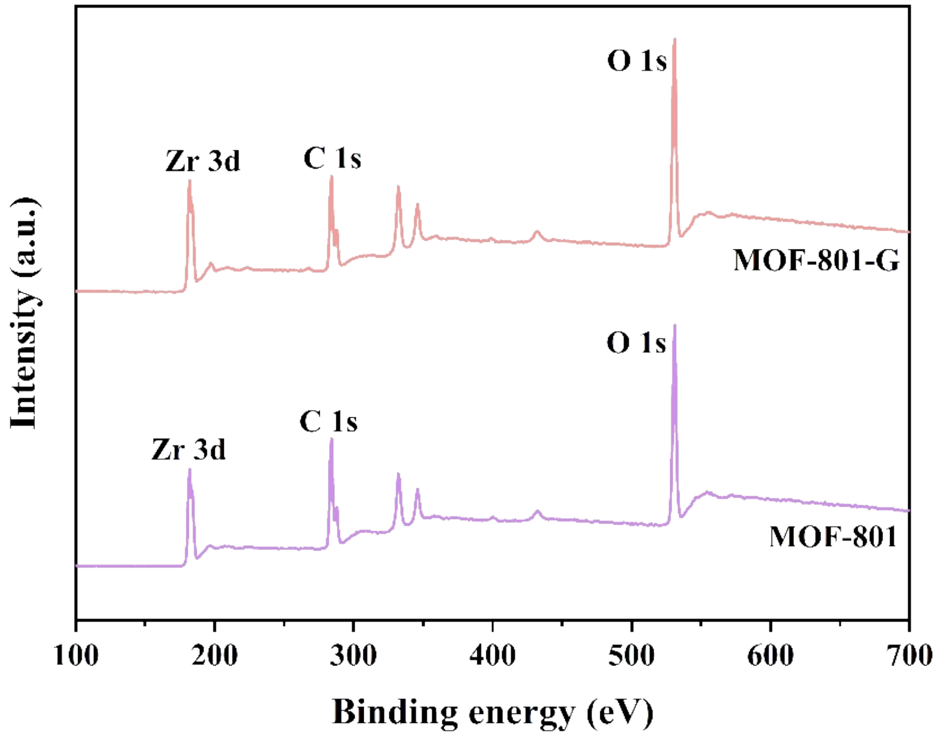

Figure S1. XPS survey spectra of MOF-801 and MOF-801-G

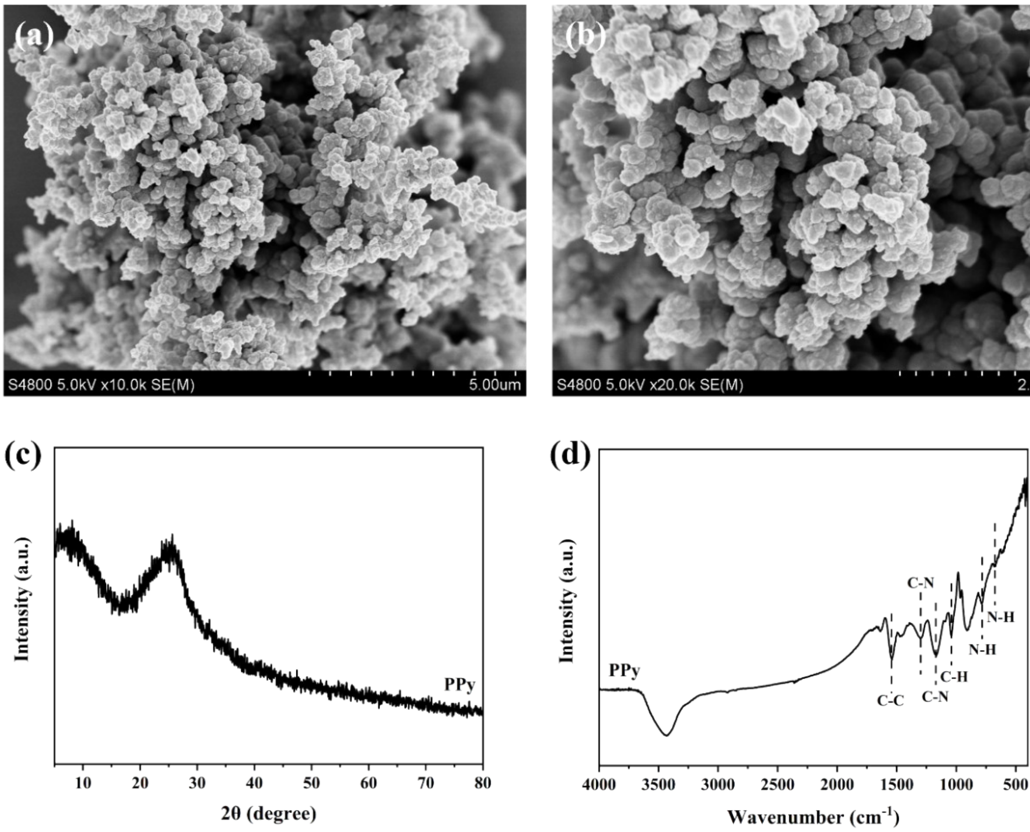

Figure S2. (a-b) SEM images, XRD, and FTIR of PPy.

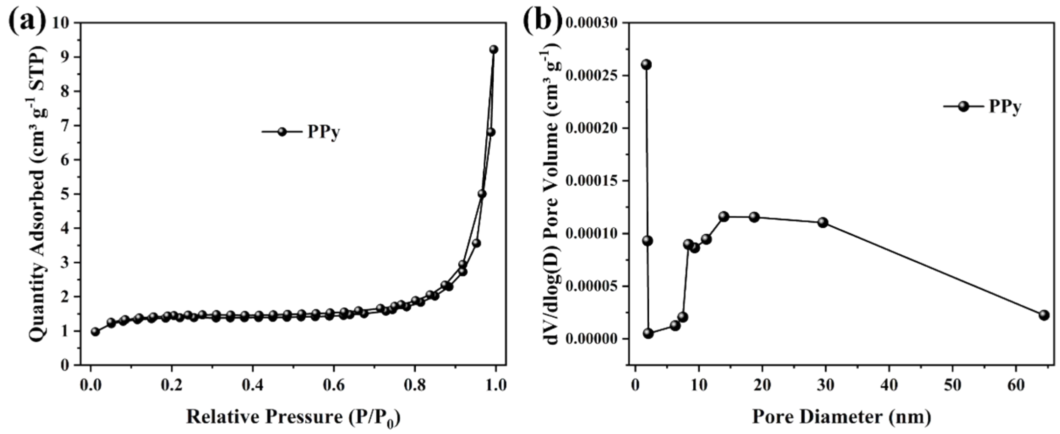

Figure S3. (a) N_2 adsorption-desorption isotherms and (b) pore size distribution of PPy.

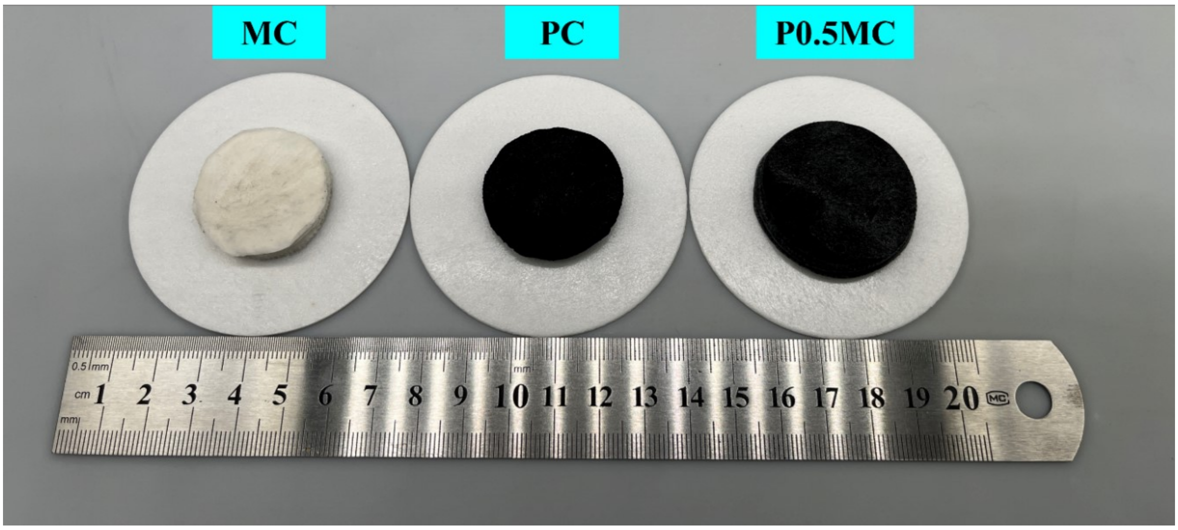

Figure S4. Digital photographs of MC, PC, and P0.5MC.

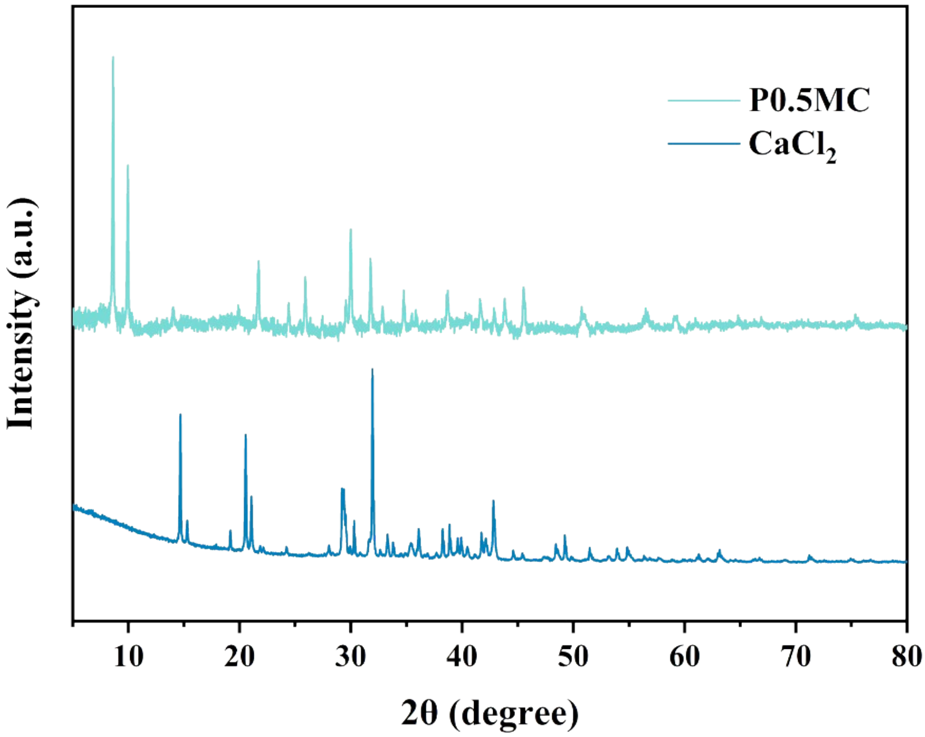

Figure S4. XRD of P0.5MC and $CaCl_2$.

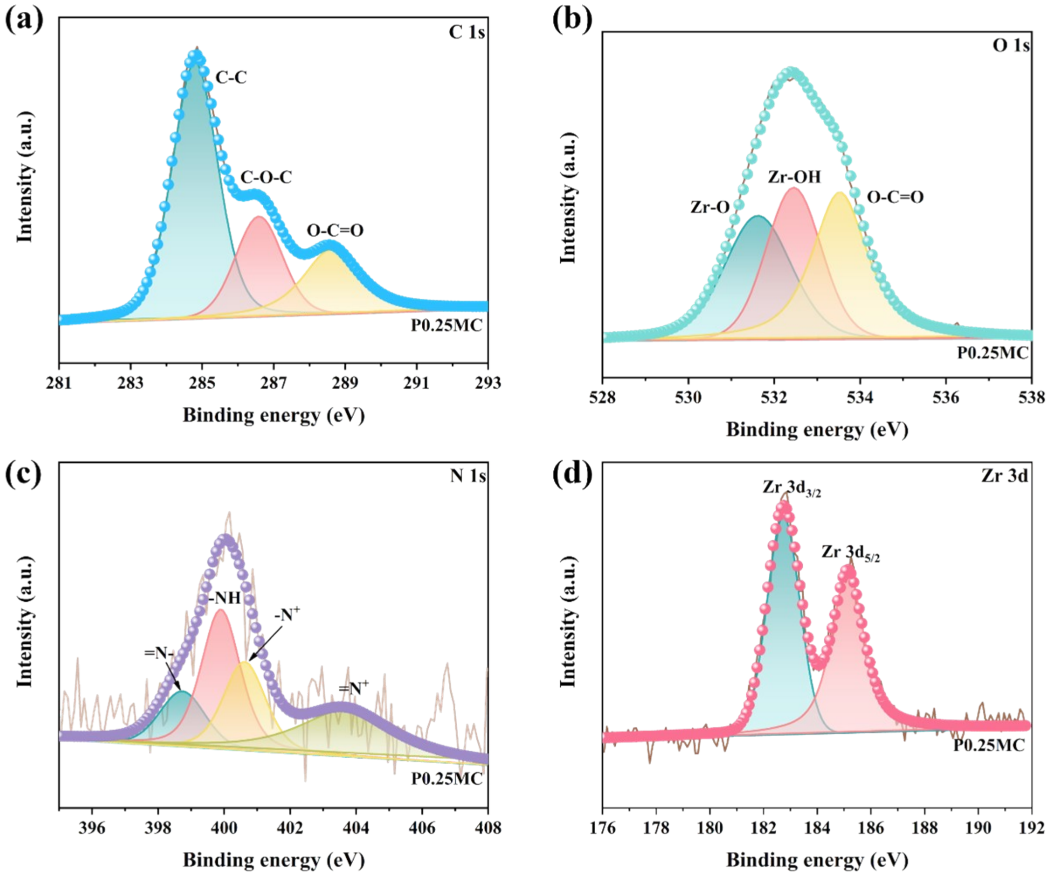

90

91 **Figure S5.** XPS spectrums of P0.25MC: (a) C 1s, (b) O 1s, (c) N 1s, and (d) Zr 3d.

92

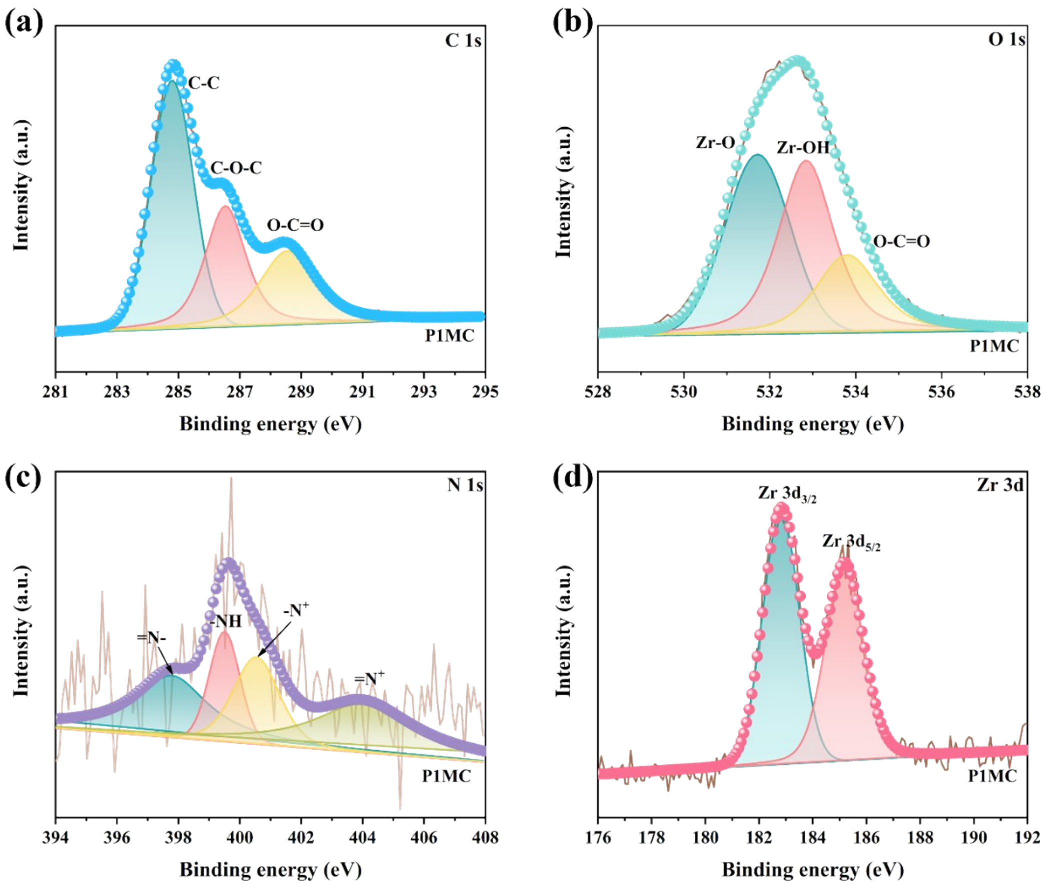

93

94 **Figure S6.** XPS spectrums of P1MC: (a) C 1s, (b) O 1s, (c) N 1s, and (d) Zr 3d.

95

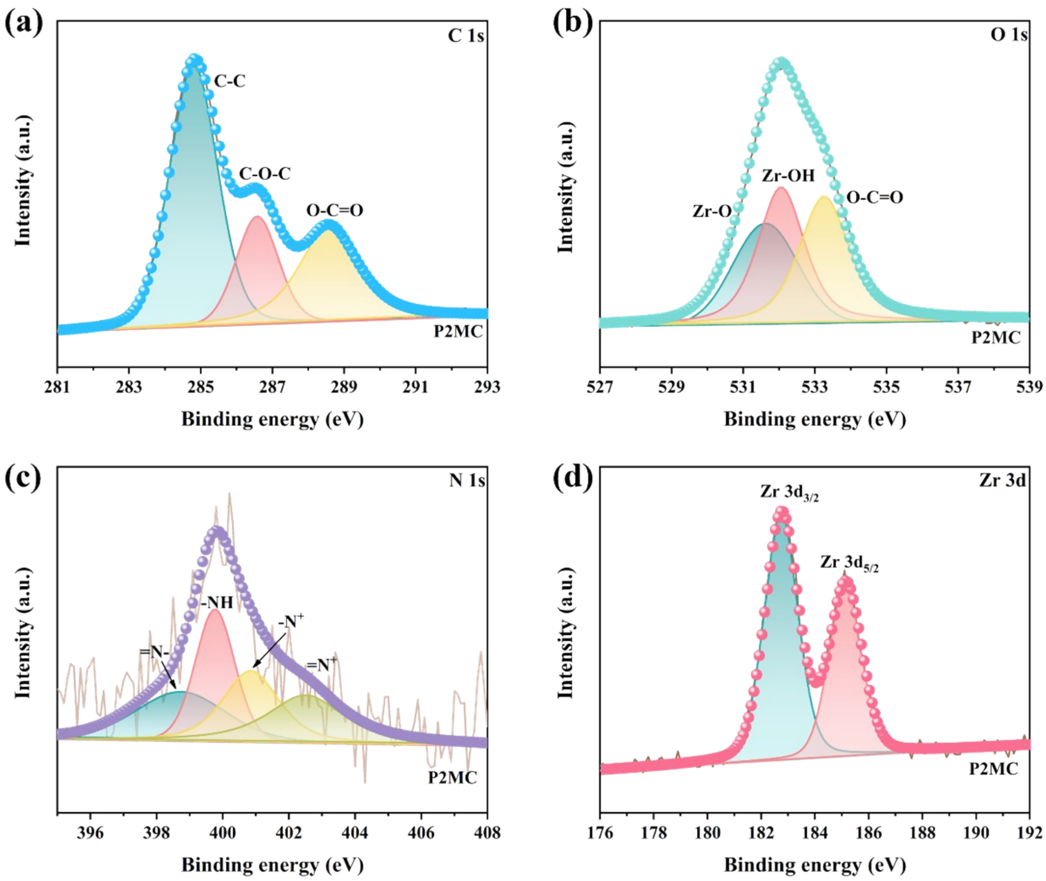

Figure S7. XPS spectrums of P2MC: (a) C 1s, (b) O 1s, (c) N 1s, and (d) Zr 3d.

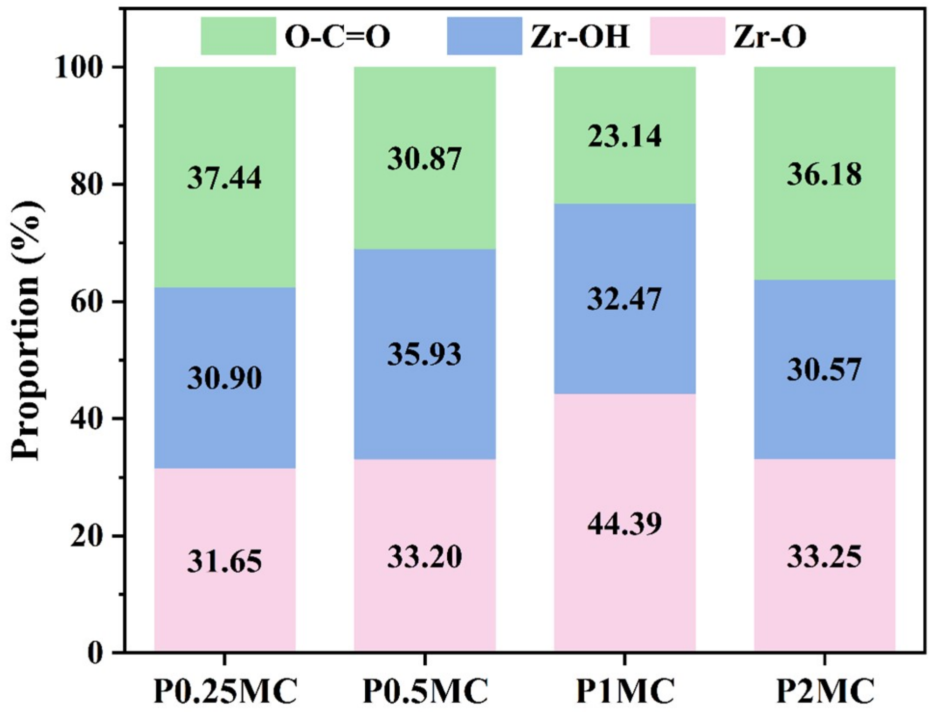

Figure S8. The ratio of oxygen species in the sample.

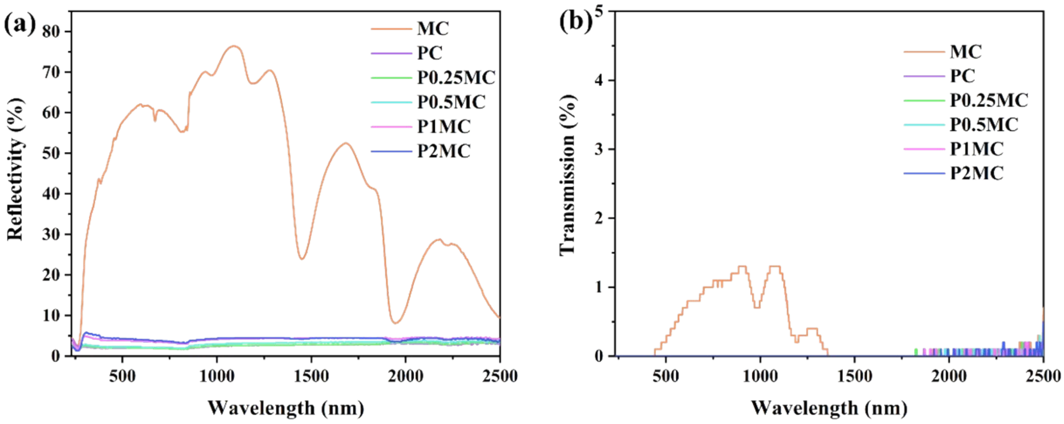

Figure S9. UV-Vis-NIR spectra of MC, PC, P0.25MC, P0.5MC, P1MC, and P2MC: (a) reflectivity and (b) transmission.

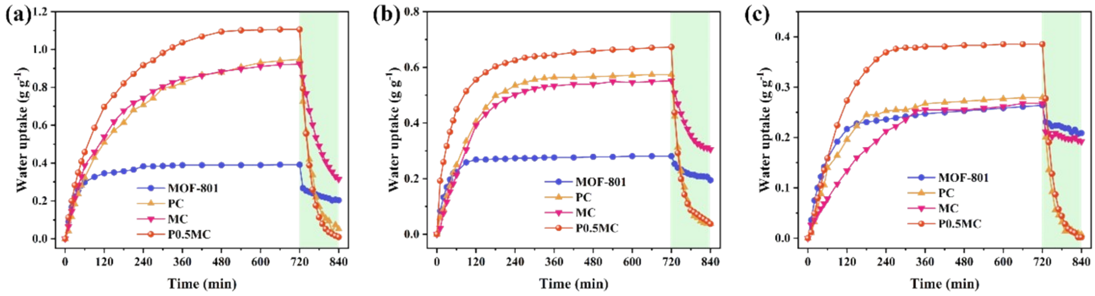

Figure S10. Water uptake of P0.5MC for AWH at 25 °C and (a) 60% RH, (b) 40% RH and (c) 20% RH.

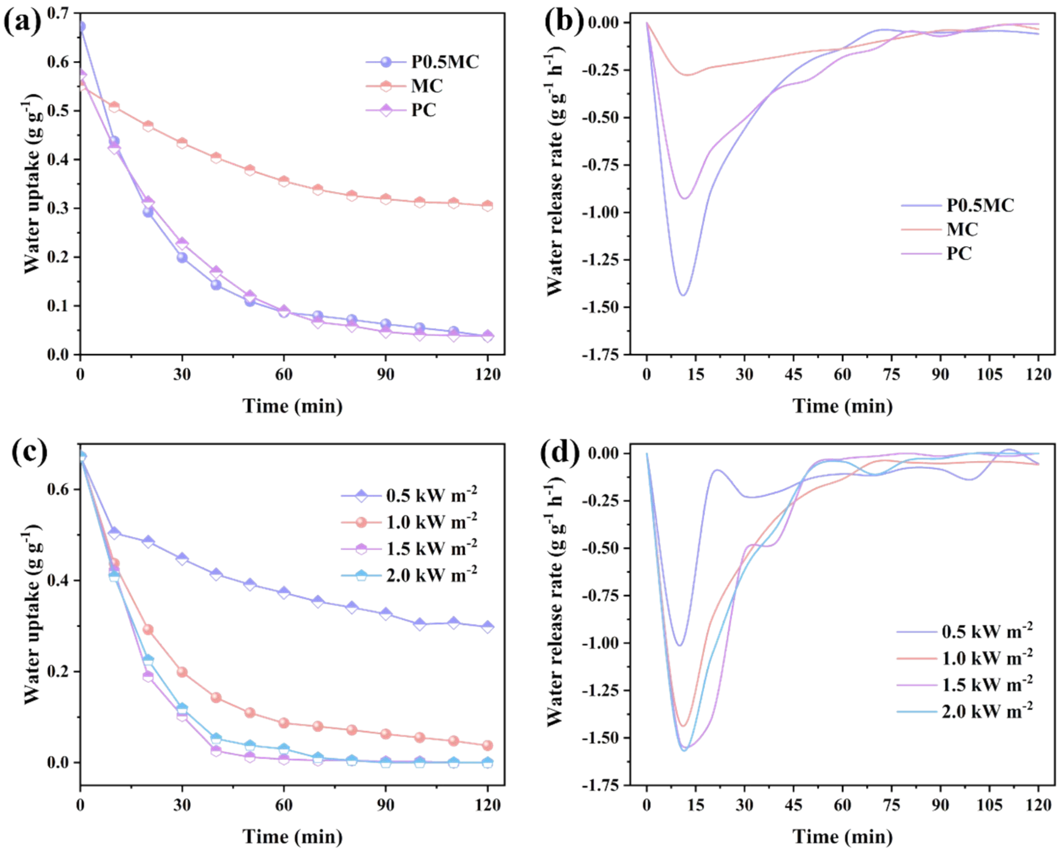

109

110 **Figure S11.** (a) Mass during desorption and (b) water release rate of MC, PC, and P0.5MC under 1.0 kW

111 m^{-2}. (c) Mass during desorption and (d) water release rate of P0.5MC under different light intensities.

112

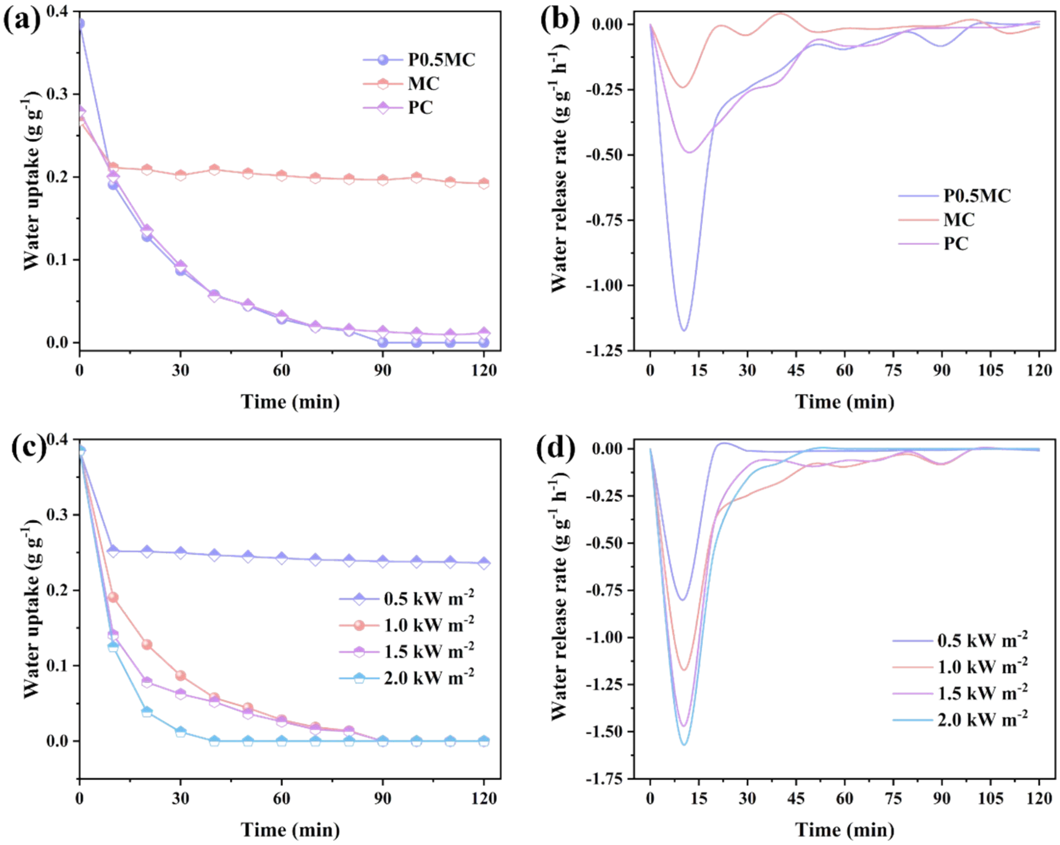

Figure S12. (a) Mass during desorption and (b) water release rate of MC, PC, and P0.5MC under 1.0 kW m^{-2}. (c) Mass during desorption and (d) water release rate of P0.5MC under different light intensities.

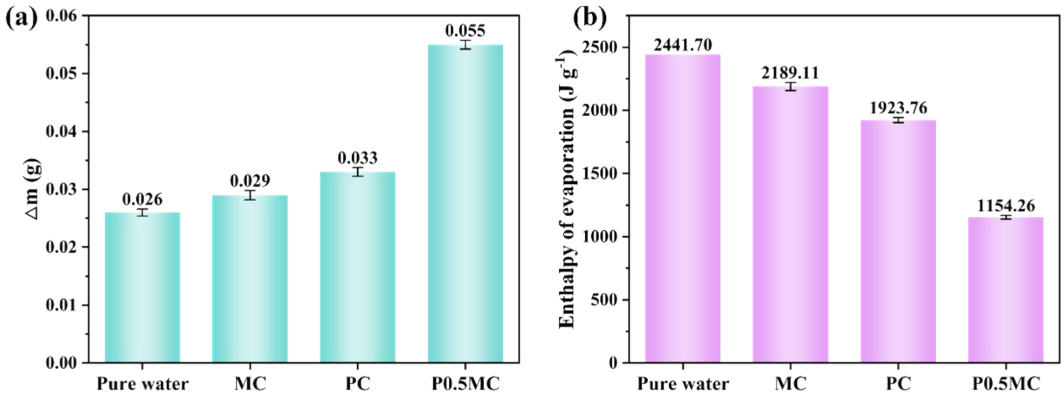

Figure S13. (a) Mass change of pure water, MC, PC, and P0.5MC in dark condition after 1 h. (b) Evaporation Enthalpy of pure water, MC, PC, and P0.5MC.

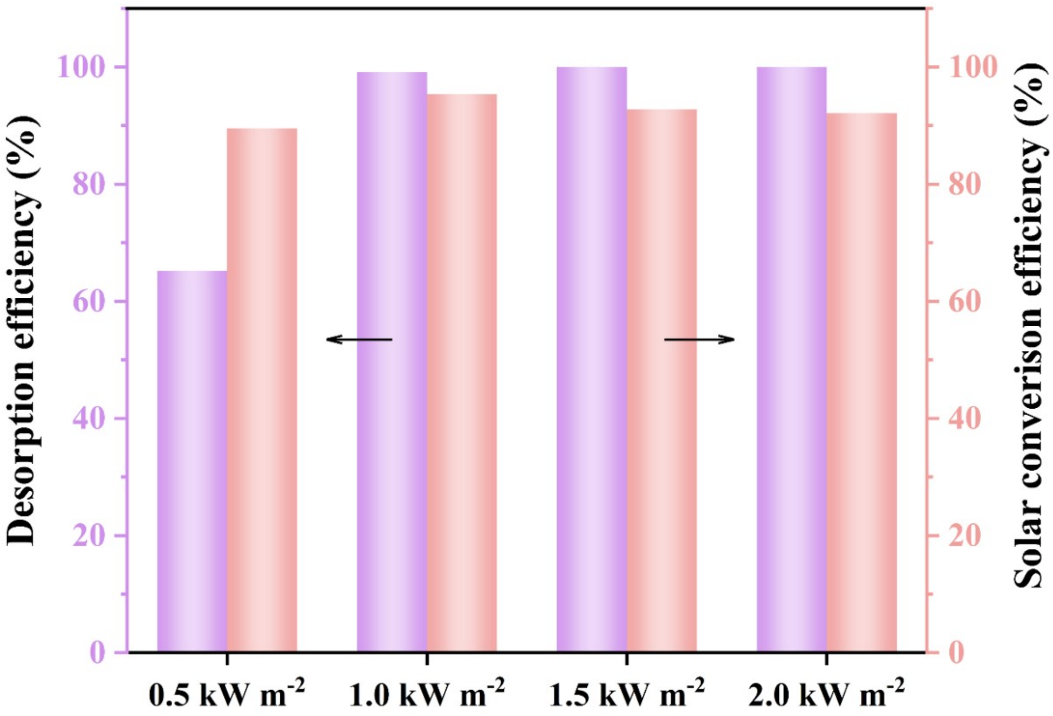

Figure S14. The desorption efficiency and the solar conversion efficiency

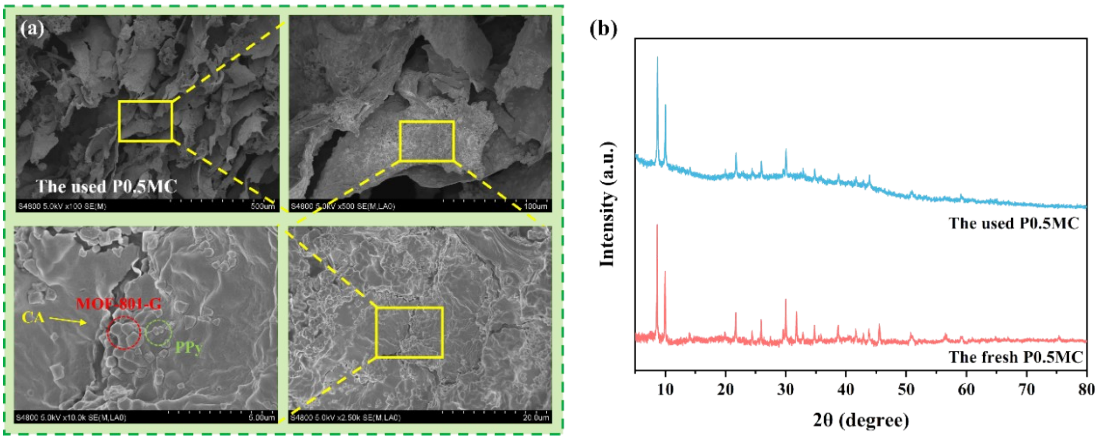

Figure S15. (a) SEM images of the used P0.5MC. (b) XRD spectrums of the fresh P0.5MC and the used P0.5MC.

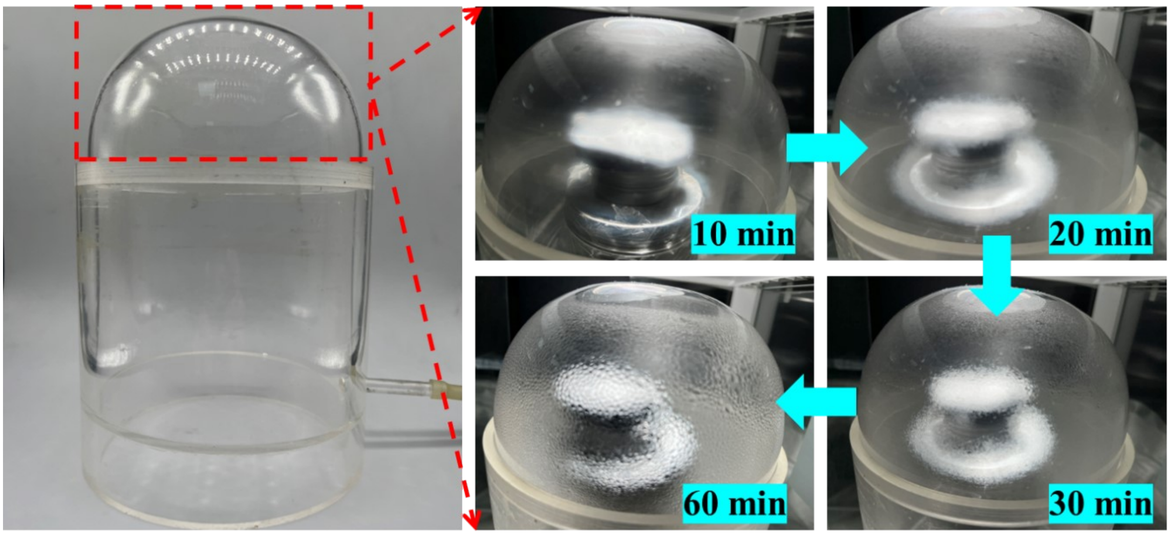

Figure S16. Photographs of the small device (Quartz Rounded Top) used for the AWH experiment and the process of water droplet formation on the walls of the device.

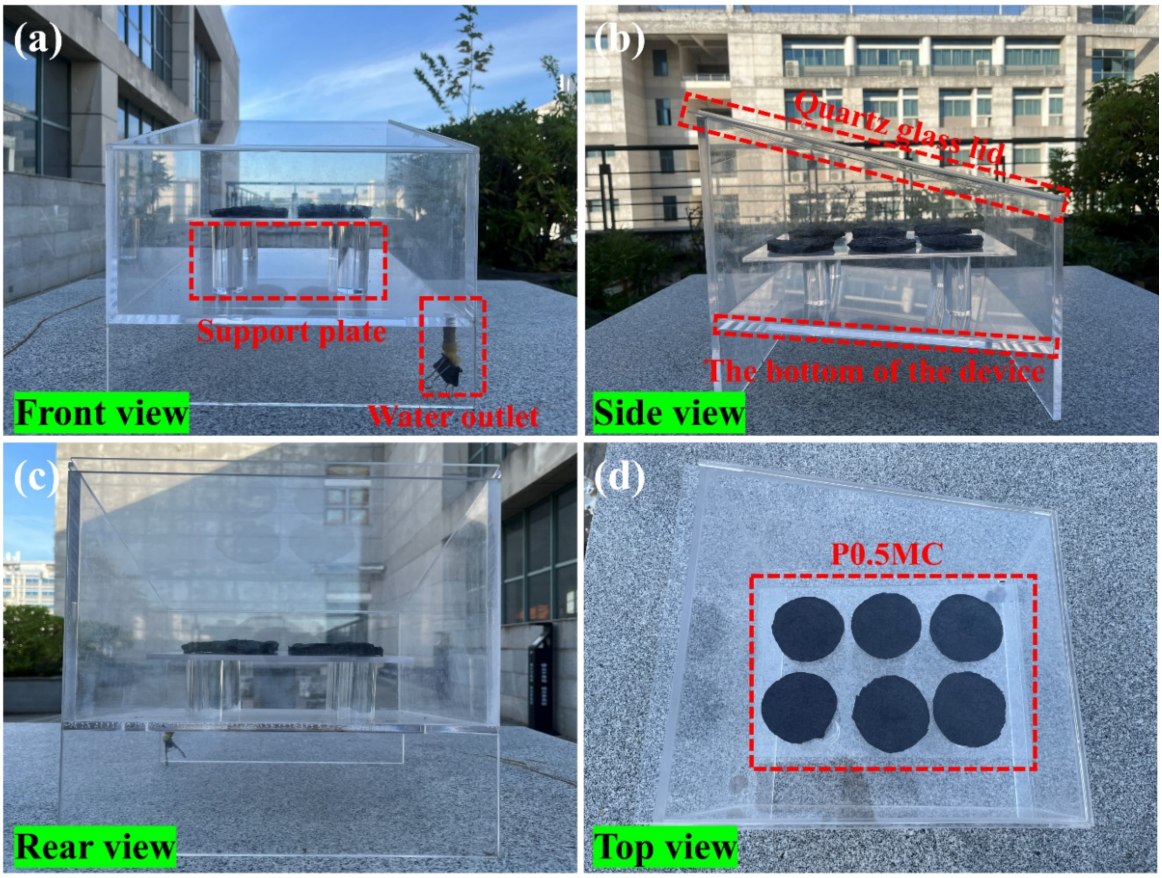

Figure S17. Outdoor water harvesting device diagram: (a) Front view, (b) Side view, (c) Rear view, and (d) Top view.

Figure S18. Cloudy skies between 7:00 a.m.-10:00 a.m. on July 7, 2024.

Table S1. Comparison of light absorption of different absorbent materials in the wavelength range of 230-2500 nm.

Sample	Total light absorption	UV absorption (230-400 nm)	Visible light absorption (400-760 nm)	Near-infrared light absorption (760-2500 nm)
MC	55.72%	56.74%	41.63%	75.08%
PC	97.44%	97.24%	98.30%	97.60%
P0.25MC	97.39%	97.18%	98.28%	97.76%
P0.5MC	96.95%	96.67%	98.04%	97.46%
P1MC	95.88%	95.70%	96.61%	96.18%
P2MC	95.84%	95.76%	96.19%	95.89%

Samples	Water uptake (g g^{-1})			Ref.
	20% RH	40% RH	60% RH	
P0.5MC aerogel	**0.387**	**0.673**	**1.106**	**This work**
MOF-801 powder	0.080	0.160	—	4
MOF-801 powder	0.225	0.295	—	5
MOF-801 powder	0.215	0.225	0.305	6
MOF-801 powder	0.295	0.305	0.315	7
MOF-801 powder	0.145	0.150	0.160	8
MOF-801 powder	0.195	0.205	0.215	9
MOF-801-hydrazine powder	0.305	0.375	0.400	6
MOF-801@P(NIPAM-GMA) gel	0.315	0.375	0.415	8
MOF-801/PPG gel	0.295	0.310	0.400	10

Table S2. Comparison of water absorption of different hygroscopic agents.

References

1. B. Ghalei, K. Wakimoto, C. Y. Wu, A. P. Isfahani, T. Yamamoto, K. Sakurai, M. Higuchi, B. K. Chang, S. Kitagawa and E. Sivaniah, *Angewandte Chemie International Edition*, 2019, **58**, 19034-19040.
2. T. H. Lee, J. G. Jung, Y. J. Kim, J. S. Roh, H. W. Yoon, B. S. Ghanem, H. W. Kim, Y. H. Cho, I. Pinnau and H. B. Park, *Angewandte Chemie International Edition*, 2021, **60**, 13081-13088.
3. G. C. Shearer, S. Chavan, S. Bordiga, S. Svelle, U. Olsbye and K. P. Lillerud, *Chemistry of Materials*, 2016, **28**, 3749-3761.
4. G. Tao, X. Chen, Y. Wang, Z. Ding, D. Wang, J. Wang, J. Ding, X. Wang, Z. Cheng and L. Cheng, *Journal of Cleaner Production*, 2023, **419**, 138296.
5. Y. Hu, Y. Wang, Z. Fang, X. Wan, M. Dong, Z. Ye and X. Peng, *Journal of Materials Chemistry A*, 2022, **10**, 15116-15126.
6. X. Yan, F. Xue, C. Zhang, H. Peng, J. Huang, F. Liu, K. Lu, R. Wang, J. Shi, N. Li, W. Chen and M. Liu, *EcoMat*, 2024, **6**, e12473.
7. H. Kim, S. Yang, S. R. Rao, S. Narayanan, E. A. Kapustin, H. Furukawa, A. S. Umans, O. M. Yaghi and E. N. Wang, *Science*, 2017, **356**, 430-434.
8. C. Yang, H. Wu, J. Yun, J. Jin, H. Meng, J. Caro and J. Mi, *Advanced Materials*, 2023, **35**, 2210235.
9. Y. Lv, J. Wu, J. Dong and T. Jia, *Journal*, 2024, **14**, 472.
10. Y. He, T. Fu, L. Wang, J. Liu, G. Liu and H. Zhao, *Chemical Engineering Journal*, 2023, **472**, 144786.